

Determination of Diltiazem Hydrochloride using Paper-based ECL sensor

Hilal TORUL ^{1*} 

¹ Department of Analytical Chemistry, Faculty of Pharmacy, Gazi University, Ankara, Turkey.

* Corresponding Authors. E-mail: hilaltorul@gazi.edu.tr (H.T.); Tel. +90 312 202 3100. Fax: +90 312 223 50 18

Received: 22 June 2022 / Revised: 01 August 2022 / Accepted: 07 August 2022

ABSTRACT: In this study, a paper-based electrochemiluminescence (ECL) sensor was developed for the determination of diltiazem hydrochloride (DTZ-HCl), which is a vasodilator of the calcium channel blocker. Herein, the ability of DTZ to act as a co-reactant for Ru(bpy)₃²⁺ in the ECL system was utilized. The pharmaceutical dosage forms were studied to verify the applicability of the developed ECL method. A paper electrode was fabricated by mimicking commercial screen-printed electrodes (SPE) and decorated with gold nanoparticles by using an electrodeposition technique in order to enhance the ECL signals. To generate the excited states of the Ru-(bpy)₃²⁺/DTZ-HCl pair, the potential in a range from -0.5 to 1.3 V at a scan rate of 100 mV/s was applied by utilizing cyclic voltammetry (CV) to the gold nanoparticle decorated paper electrode (AuNPs@PE). The ECL signals were recorded using the μStat ECL potentiostat, which is controlled by DropView 8400 Software, concurrently. The coefficient of determination and limit of detection obtained from the standard addition method were found as 0.997 and 0.12 μg/mL, respectively. Furthermore, the usage of conventional SPE electrodes confirmed that the results obtained by the developed method were acceptable with the similarity of 97.2% in terms of average recovery value, for the detection of DTZ-HCl in pharmaceutical dosage forms. This study is a startup method to develop highly selective paper-based ECL sensors in routine drug analysis that is fast and low cost.

KEYWORDS: electrochemiluminescence; ECL; paper electrode; diltiazem; pharmaceutical

1. INTRODUCTION

Diltiazem (DTZ) is a crucial vasodilator of the calcium channel blocker. DTZ treats hypertension, and arrhythmia, by inhibiting calcium influx into the muscles and coronary arteries during depolarization [1, 2]. Furthermore, DTZ is known to be used in angina treatment [3]. It is important to monitor DTZ levels since the overdose of DTZ may cause a slow heartbeat, chest pain, hypotension, and fainting. Moreover, it can lead to death in patients who have sick sinus syndrome for long-term usage [4, 5]. Although the determination of DTZ is carried out by high-performance liquid chromatography (HPLC) recommended by the United States Pharmacopoeia [6], furthermore, several studies have been reported in the literature regarding the use of various techniques such as gas chromatography [7], liquid-liquid microextraction [8], capillary electrophoresis [9], Raman spectroscopy [10], colorimetry [11], spectrophotometry [12], and electrochemical sensors [3–5]. Despite several advantages such as high sensitivity and selectivity in low concentrations of DTZ, these powerful techniques have some limitations such as the requirements of high-volume samples, expensive equipment, skilled personnel, and time-consuming procedures [3, 5]. At this point, electrochemical sensors have an interest in a lot of attention because of their unique properties such as short analysis time, low-cost instrumentation, and analysis. They also provide an opportunity for accurate, selective, and sensitive analysis with a small volume of samples [13, 14].

Electrochemiluminescence, also known as electrogenerated chemiluminescence, is a form of light emission in which certain molecules perform an exergonic electron transfer reaction at the working electrode surface. An electrochemically produced light emission obtained by applying a required voltage to the electrode surface in the presence of a luminophore or luminophore/co-reactant pair is defined as the ECL approach. Depending on the radical source, ECL can be categorized into annihilation and co-reactant mechanisms. While a luminophore produces radicals in the annihilation mechanism, radicals are formed in the co-reactant mechanism as a consequence of electrochemical reactions between a luminophore and a co-reactant [15–17]. Because of its great attributes such as high selectivity, sensitivity, low background signal,

How to cite this article: Torul H, Determination of Diltiazem Hydrochloride using Paper-based ECL sensor. J Res Pharm. 2022; 26(5): 1472-1483.

cost-effective analysis, and giving a quick response, ECL has come to the fore in recent years as a significant analytical approach in sensor applications [18]. ECL provides all these benefits by combining electrochemical and spectroscopic techniques. In ECL systems, nanostructures, inorganic, and organic compounds can be used as luminophores [19–21]. Tris(2,2'-bipyridine)ruthenium(II) ($\text{Ru}(\text{bpy})_3^{2+}$) is one of the most common inorganic structures, which can be used as a luminophore in ECL systems since it has some advantages such as stability, high sensitivity, and regenerative capability in ECL measurement [22]. Various co-reactants, including secondary or tertiary alkylamines, amine-functionalized materials, and amino acids can be used to generate the ECL of $\text{Ru}(\text{bpy})_3^{2+}$ [23–25].

Paper-based sensors exhibit excellent compatibility with several applications as analytical supports because of their numerous properties such as being low-cost, providing eco-friendly behavior, ease to use, flexible, having porous structure, disposable, and biodegradable. They also enable the analysis with a small volume of samples [14, 26]. Several techniques have been reported in the literature, which are combined with paper-based sensors. They all have advantages and limitations [27]. Recently, there has been increased interest in the usage of paper-based sensors in ECL applications. [28].

To enhance ECL signals, various amplification strategies including enzyme catalysis, DNA amplification techniques, rolling circle amplification (RCA), enzyme catalysis, and nanomaterials have been developed [29, 30]. In this study, a nanomaterial-based enhancement strategy was benefited, and the paper electrodes were decorated with gold nanoparticles (AuNPs). AuNPs enable significant signal amplification in ECL signals by utilizing benefits such as catalytic effect, dielectric characteristics, and high electron density [31, 32]. A prevalent phenomenon known as plasmon-enhanced ECL has recently received much attention in the literature. Based on this phenomenon, a local surface plasmon resonance (LSPR), in which free electrons collectively vibrate in metal nanostructures inspired by an electromagnetic (EM) field, has provided a significant improvement in the ECL signal intensities [30, 31].

In this study, a paper-based ECL sensor was fabricated for the determination of diltiazem hydrochloride (DTZ-HCl) for the first time in the literature. Herein, the ability of DTZ to act as a co-reactant for $\text{Ru}(\text{bpy})_3^{2+}$ in the ECL system was utilized. For the demonstration of the applicability of the developed methodology, the detection of DTZ-HCl in pharmaceutical dosage forms was achieved by monitoring the ECL of $\text{Ru}(\text{bpy})_3^{2+}$ in the presence of DTZ.

2. RESULTS

We fabricated and used the PEs for several applications in our previous studies [13, 14, 33, 34]. Here, the PE was utilized as an ECL sensor for the determination of DTZ-HCl. The point of this study is that the detection of the DTZ-HCl is achieved by utilizing the ability of DTZ to act as a co-reactant for $\text{Ru}(\text{bpy})_3^{2+}$ in the ECL system. Initially, a PE was fabricated and modified the surface of the WE with AuNPs to enhance the ECL signals. After the characterization studies, the optimization studies of the developed system were carried out. Then, the detection of DTZ-HCl in pharmaceutical dosage forms was achieved by monitoring the ECL of $\text{Ru}(\text{bpy})_3^{2+}$ in the presence of DTZ. The obtained results were detailed in the following sections.

2.1. The characterization of the AuNPs@PE

In this study, carbon paste which has relatively low conductivity was used to fabricate the three-electrode system of the PEs. The PEs were decorated with AuNPs to enhance their conductivity. The electrochemical behaviors of the electrodes were monitored using CV in 5.0 mM $[\text{Fe}(\text{CN})_6]^{3-/4-}$ containing 0.1 M KCl. After the modification of PEs with AuNPs, the anodic and cathodic currents of the redox probe on the PE surface increased considerably.

The Randles–Sevcik equation (Eq), where I_p , the peak current (I_a or I_c) in A; n , the number of transferred electrons; A , the surface area in cm^2 ; D , the diffusion coefficient in cm^2/s ; C , the concentration of electroactive species in mol/cm^3 ; v , the scan rate in V/s . was used to estimate the electroactive surface areas of the PEs.

$$I_p = 2.687 \times 10^5 \times n^{3/2} \times A \times D^{1/2} \times C \times v^{1/2} \quad (\text{Eq})$$

Based on I_a , the areas of unmodified PE and AuNPs@PE were determined to be 0.056 cm^2 and 0.129 cm^2 , respectively. The AuNPs improved the electroactive surface area of the PE by 130 percent, increasing the sensitivity of AuNPs@PE. The results demonstrated an increase in electron transfer and the surface area.

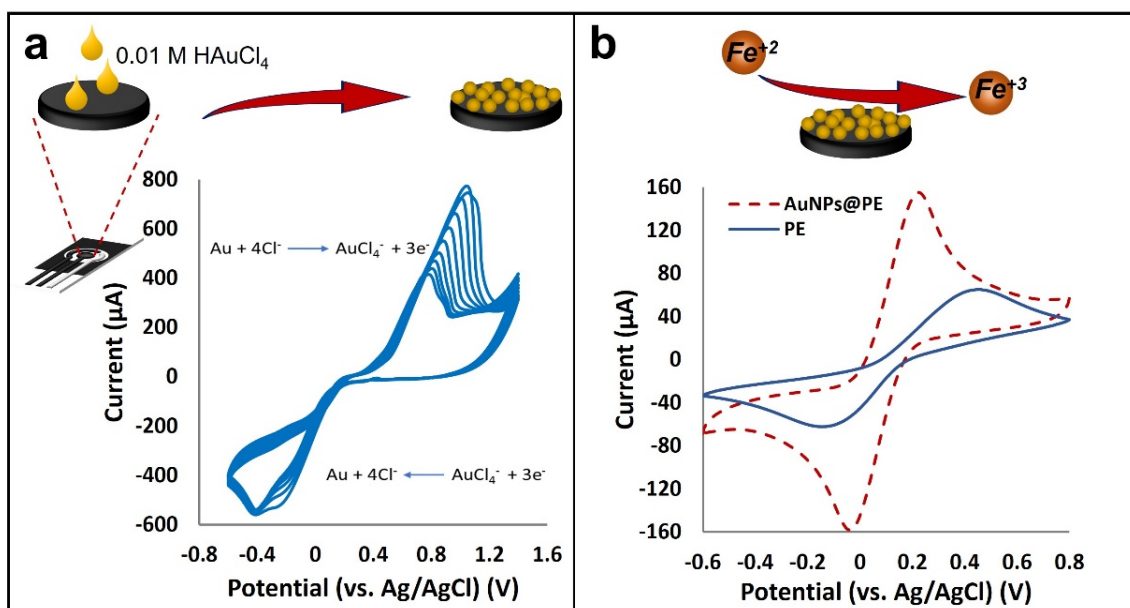


Figure 1. a) The modification procedure of paper electrodes using CV, from 10.0 mM HAuCl₄ in 100.0 mM KCl and 100.0 mM H₂SO₄, on the WE for 10 cycles at a scan rate of 0.2 V/s in the range of -0.6 to +1.4 V, b) cyclic voltammograms of bare (PE) and modified with AuNPs (AuNPs@PE) for 5.0 mM [Fe(CN)₆]^{3-/4-} in 0.1 M KCl at a scan rate of 0.1 V/s.

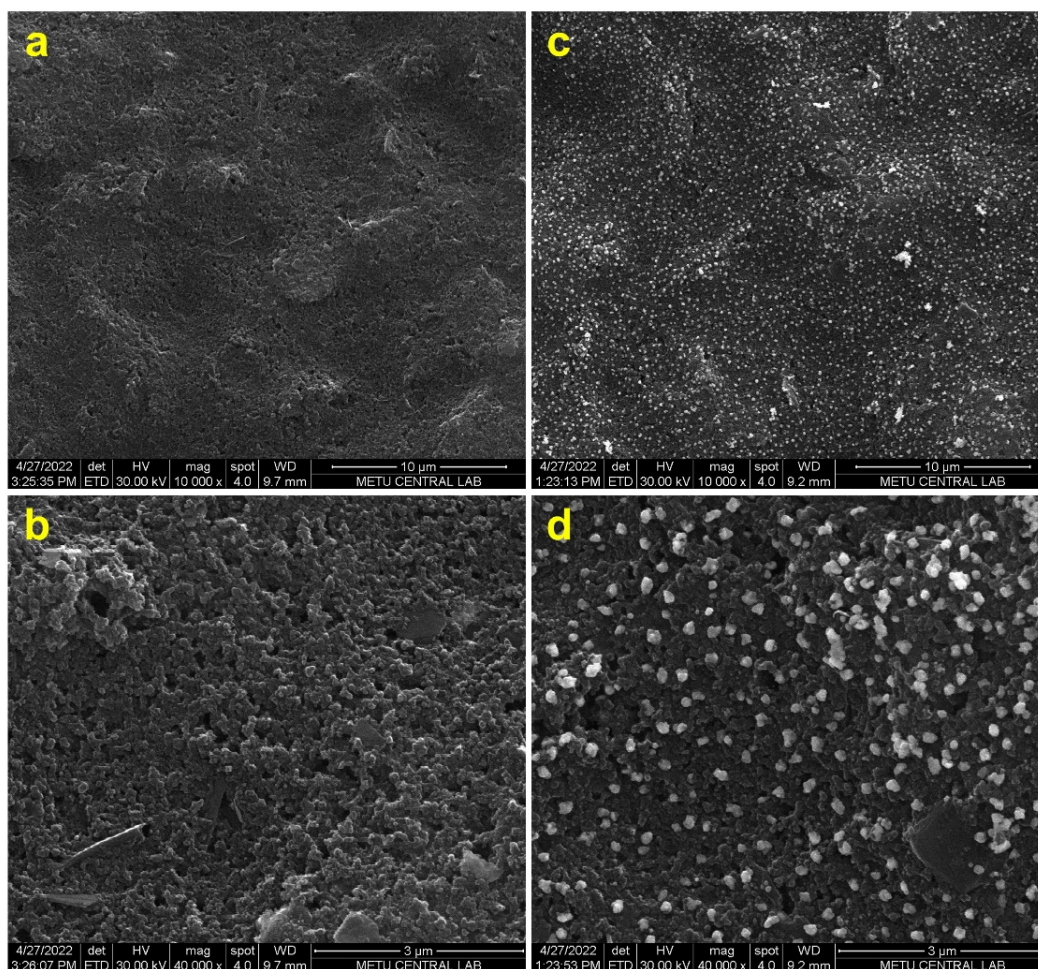


Figure 2. SEM images of bare and AuNP modified paper electrodes at 10000× magnification (a, c) and 40000× magnification (b, d), respectively

To characterize the morphologies of unmodified and AuNPs modified PEs, SEM analysis was used, as well. SEM images of the electrodes were recorded after covering them with sputtering gold. Figures 2a and b show the penetration of carbon paste into the porous NC membrane. As shown in Figures 2c and d, the electrodeposition of AuNPs was achieved successfully. It was observed that the AuNPs were synthesized with a uniform distribution on the WE surface. According to SEM images, the average size of the particles was found as 152 ± 18 nm and the particle density was found as 6.2×10^6 particle/mm².

2.2. Optimization studies for the paper-based ECL sensor

The ECL intensity is mostly determined by the concentrations of the luminophore and co-reactant. Besides, several parameters such as the surface modification of the electrode, the ambient pH, scanning voltage range, and scan rate are also crucial in increasing ECL intensities. All these parameters were optimized to enhance the signals in the paper-based ECL sensor. The electrodeposition parameters of the AuNPs were optimized by applying different numbers of cycles and scan rates. Following the optimization studies, it was decided to perform the deposition of particles by using CV in a potential range between -0.6 and +1.4 V at a scan rate of 200 mV/s for 10 cycles (Data not shown).

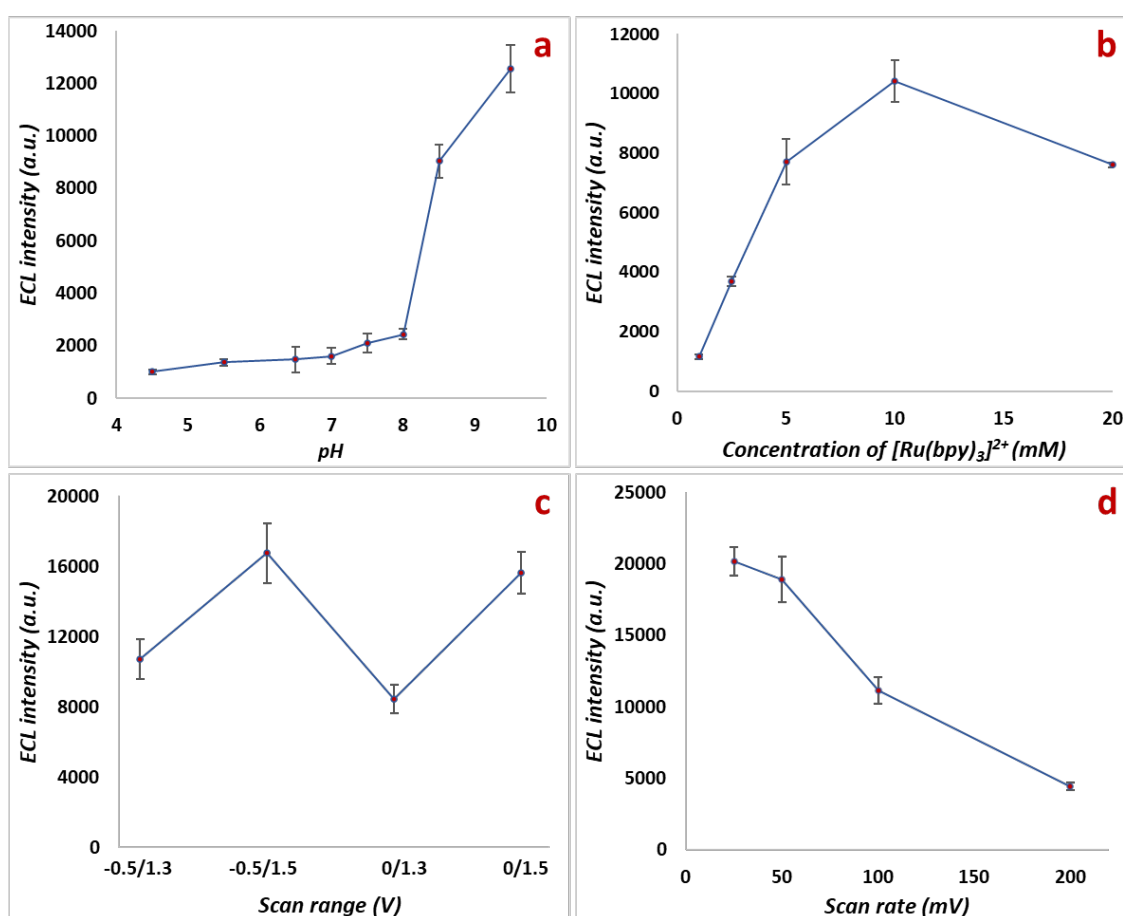


Figure 3. The effect of a) pH of the electrolyte solutions, b) the concentration of the $Ru(bpy)_3^{2+}$ solution in the range from 1.0 to 20.0 mM, c) the different scanning potential ranges between -0.5/1.3V, -0.5/1.5V, 0/1.3 V, and 0/1.5 V, d) scan rates of 25, 50, 100, and 200 mV/s on ECL signals of 10.0 mM $Ru(bpy)_3^{2+}$ in the presence of 100.0 $\mu\text{g/mL}$ DTZ

The ambient pH is not only important to enhance the ECL signal intensities, but also to provide the stability of luminophore. Therefore, the effect of pH on the ECL signal intensity of $Ru(bpy)_3^{2+}/DTZ$ was investigated by varying the pH of the buffer solution from 4.5 to 9.5. While performing the experiments, it was observed that the stability of the ruthenium luminophore remains unaffected at relatively low and high pH ranges. Moreover, the ECL intensities increased after the pH 8. As a result, the maximum ECL signals were recorded at pH 9.5 (Figure 3a).

The change of the ECL signals based on the concentration of the $Ru(bpy)_3^{2+}$ solution was evaluated under various concentrations from 1.0 to 20.0 mM (n:5). As the concentration of $Ru(bpy)_3^{2+}$ was increased, the

ECL intensity of Ru-(bpy)₃²⁺/DTZ increased, as well. However, a decrease was observed in the signal intensity after 10.0 mM Ru-(bpy)₃²⁺. Accordingly, it was decided to use 10.0 mM Ru-(bpy)₃²⁺ to generate the ECL signals.

To evaluate the effect of different scanning potential ranges on ECL signal intensities, four different scanning potential ranges between 0/1.3 V, -0.5/1.3 V, 0/1.5 V, and -0.5/1.5 V were investigated using 10.0 mM Ru-(bpy)₃²⁺ and 100.0 µg/mL DTZ solutions. Although peak intensities increased in the high scanning potential ranges, peak splitting was observed, which is related to the various possible types of radicals produced by the reaction of Ru-(bpy)₃²⁺/DTZ, as shown in Figure 3c. The scanning potential range of -0.5 to 1.3 V provided the optimum ECL signal.

Since the ECL intensities depend on the scan rate, four different scan rates of 25, 50, 100, and 200 mV/s were also investigated by using CV in the potential between -0.5 and +1.3 V. As shown in Figure 3d, a decrease was observed in the signal intensity by the increasing the scan rates. Because analysis time was relatively long when working at 25 and 200 mV/s scanning rates, it was decided to work at 100 mV/s. After overall optimization studies, the ECL of Ru-(bpy)₃²⁺/DTZ was generated in the presence of 10.0 mM Ru-(bpy)₃²⁺ in pH 9.5 TRIS buffer and the DTZ sample, by using CV at a scan rate of 100 mV/s in the range of -0.5 to +1.3 V for 5 cycles.

2.3. Analytical performance of the paper-based ECL sensor

The method characteristics such as the linear range, the LOD, sensitivity, precision, and accuracy were evaluated to determine the analytical performance of the proposed paper-based ECL sensor for the detection of DTZ-HCl. Herein, the determination of DTZ-HCl was achieved using the PEs fabricated in our lab and commercial screen-printed electrodes (SPE). The standard solutions of DTZ-HCl at varying concentrations in the range from 1.0 to 100.0 µg/mL were used to indicate the linear range and the LOD values. The measurements were carried out as mentioned in section 5.4 and the ECL signals of Ru-(bpy)₃²⁺/DTZ-HCl were obtained under optimized conditions. A linear relationship between ECL intensity and DTZ-HCl concentration was observed for both PE and SPE with coefficients of determination (R²) of 0.9970 and 0.9924, respectively. Using the equation LOD = 3s/m, where m is the slope of the calibration plot and s is the standard deviation of the intercept, the limit of detection (LOD) was estimated for PE and SPE-ECL sensors as 0.12 and 0.28 µg/mL, respectively.

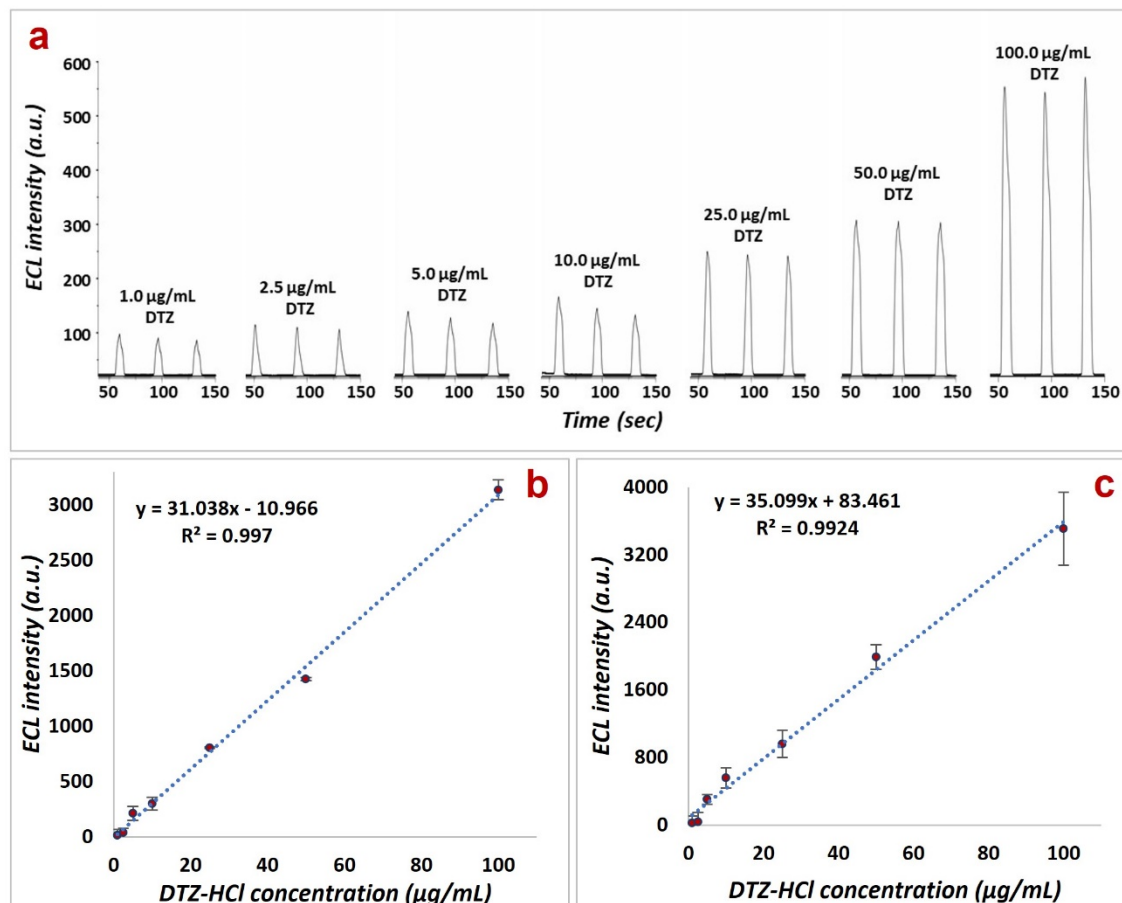


Figure 4. a) The ECL signals of Ru-(bpy)₃²⁺ in the presence of DTZ-HCl at varying concentrations from 1.0 to 100.0 µg/mL, using the paper-based ECL sensor. The calibration plots obtained from the variation in the ECL signals at different concentrations of DTZ-HCl from 1.0 to 100.0 µg/mL, **b)** using the paper-based ECL sensor, and **c)** SPE-ECL sensor, at a scan rate of 0.1 V s⁻¹, from -0.5 V to 1.3 V

DTZ-HCl was detected in pharmaceutical dosage forms prepared at three different concentrations of 30.0, 40.0, and 50.0 µg/mL, as indicated in section 5.4, to verify the applicability of the proposed method to real samples. Accordingly, the measurement was performed to obtain the ECL signals of Ru-(bpy)₃²⁺/DTZ-HCl using both PE and SPE ECL sensors. For each sample, the measurements were repeated three times. The recovery values of DTZ-HCl in pharmaceutical drug samples were calculated based on calibration data and found as 96.8%, 100.5%, and 99.3%. The SPE-ECL sensor was also used to detect DTZ-HCl in pharmaceutical drug samples as a comparative sensor. The method parameters were provided in Table 1. According to the results, the proposed method was confirmed to be reliable and reproducible. Ultimately, the results demonstrated that the proposed method could be used to detect DTZ-HCl in pharmaceutical dosage forms. The average recovery of DTZ-HCl was found as 98.9% using the paper-based ECL sensor. The SPE-ECL sensor confirmed that the developed method was applicable for the DTZ-HCl detection in pharmaceutical formulations with a similarity of 97.2% in terms of recovery values.

Table 1. The comparison of the paper-based ECL sensor and the commercial SPE for the DTZ-HCl detection in (n=3)

Paper-based electrode				Commercial screen printed electrode		
Sample ($\mu\text{g/mL}$)	Found ($\mu\text{g/mL}$)	Recovery %	Parameters	Found ($\mu\text{g/mL}$)	Recovery %	Parameters
30.0	29.05 \pm 0.70	96.8	\bar{x} = 98.9 ^a SD = 1.52	30.9 \pm 1.74	102.9	\bar{x} = 101.7 ^a SD = 1.41
40.0	40.20 \pm 0.93	100.5	RSD, % = 1.54 CI = 102.6 - 95.1 ^b	41.0 \pm 1.20	102.5	RSD, % = 1.39 CI = 105.2 - 98.2 ^b
50.0	49.63 \pm 3.63	99.3	(P = 0.05)	49.9 \pm 1.04	99.7	(P = 0.05)

^a \bar{x} = Mean^b CI = Confidence interval

The method repeatability (intra-day precision) and intermediate precision (inter-day precision) were used to evaluate the precision of the developed method. While the ECL measurements were performed three times within a day for each sample to investigate the intra-day precision, the ECL measurements were carried out six times on two separate days for them to determine the inter-day precision. The obtained results were provided in Table 2. The proposed method was found to be precise, with low values of intra-and inter-day variations (RSD \leq 6%).

Table 2. The results of intra-and inter-day variability for the DTZ-HCl in pharmaceutical drug samples by the paper-based ECL sensor

Sample ($\mu\text{g/mL}$)	Intra-day precision (n=3)		Inter-day precision (n=6)	
	Found ($\mu\text{g/mL}$)	RSD	Found ($\mu\text{g/mL}$)	RSD
30.0	29.05 \pm 0.70	2.41	29.90 \pm 1.78	5.95
40.0	40.20 \pm 0.93	2.33	39.66 \pm 0.88	2.23
50.0	49.53 \pm 2.47	4.98	50.80 \pm 2.90	5.70

 \bar{x} = Mean, RSD: relative standard deviation (%)

3. DISCUSSION

To the best of our knowledge, a paper-based ECL sensor and the ability of DTZ to act as a co-reactant for Ru(bpy)₃²⁺ in the ECL system were utilized for the detection of DTZ-HCl for the first time in the literature. The detection of DTZ-HCl in pharmaceutical dosage forms was achieved by monitoring the ECL of Ru(bpy)₃²⁺ in the presence of DTZ.

The linear range and LOD of the developed paper-based ECL sensor were compared with the previously reported studies (Table 3). Although the EC methods have provided high sensitivity with low LOD values, they need a relatively high sample volume. Besides, the developed method provides a wide linear range compared to other reports. Furthermore, there is only one study for DTZ-HCl detection based on the ECL method coupled with capillary electrophoresis. However, this ECL method requires expensive equipment and skilled personnel. In Table 3, I also mentioned an HPLC-PDA method for DTZ-HCl detection. This method provided three times small LOD value compared to the presented method. However, the analysis time is at least 17 min after the sample preparation step. The advantages of the developed paper-based ECL sensor over the previously reported methods are low reagent consumption and the usage of low-cost paper-electrode. After the further improvement of the proposed paper-based ECL sensor, the developed method will provide a new and powerful analytical technique for DTZ-HCl detection in both biological and pharmaceutical samples.

Table 3. Comparison of the previously reported studies for the DTZ-HCl detection and the presented study

Method	Linear range ($\mu\text{g/mL}$)	LOD ($\mu\text{g/mL}$)	Reference
Capillary Electrophoresis-ECL	0.01 - 45.0	0.0023	[1]
Electrochemical analysis-MWCNT/PPy-PBA modified glassy carbon electrode	0.9 - 36.0	0.003	[3]
Electrochemical analysis-CPE/CdO-rGO/IL	0.0045-67.5	0.014	[5]
Electrochemical analysis-boron-doped diamond electrode	4.9 - 23.9	0.07	[4]
Colorimetric detection	12.0 - 32.0	-	[11]
HPLC-PDA analysis	0.12 - 4.84	0.04	[35]
Paper-based ECL	1.0 - 100.0	0.12	This study

4. CONCLUSION

A paper-based ECL sensor for fast and accurate DTZ-HCl detection in pharmaceutical dosage forms was proposed in this work for the first time in the literature. First, the PEs were constructed using a cost-effective screen-printing approach and then decorated with AuNPs using an electrodeposition technique to enhance ECL signals. To the best of our knowledge, a paper-based ECL sensor for DTZ-HCl detection has not been reported before. Herein, the ability of DTZ to act as a co-reactant for $\text{Ru}(\text{bpy})_3^{2+}$ in the ECL system was utilized. The suggested method was verified on a pharmaceutical drug sample, and the average recovery value for DTZ-HCl was determined to be 98.9%. The use of a low-cost paper electrode that can be easily modified is the main advantage of the presented method. Furthermore, the presented method offers a fast analysis time of about five minutes. In conclusion, the proposed method can be considered as a startup method to develop high selective paper-based ECL sensors in routine drug analysis that is fast and low cost.

5. MATERIALS AND METHODS

5.1. Reagents and Apparatus

NaCl , KCl , Na_2HPO_4 , and KH_2PO_4 were obtained from J.T. Baker (Deventer, Netherlands). $\text{K}_3\text{Fe}(\text{CN})_6$, $\text{K}_4\text{Fe}(\text{CN})_6$, NaH_2PO_4 , and HAuCl_4 were obtained from Sigma-Aldrich (St. Louis, MO, USA). Nitrocellulose (NC) membrane (Hi-flow Plus HFC07504) and DTZ-HCl were purchased from Merck (Darmstadt, Germany). Carbon paste used for the formation of working and reference electrodes was obtained from Daejoo Electronic Materials (Gyeonggi-do, South Korea). Silver/silver chloride ($\text{Ag}|\text{AgCl}$, 9:1) paste used to prepare the reference electrode, was obtained from Henkel (Düsseldorf, Germany).

μStat ECL potentiostat, which is controlled by DropView 8400 Software, (Metrohm Dropsens, UK) was used for the characterization studies and to carry out ECL measurements. The characterization of the AuNP-modified paper electrodes was carried out using Scanning Electron Microscope (SEM) analysis by a QUANTA 400F FEG SEM (Agilent Technologies, Santa Clara, CA) at 20-30 kV.

5.2. Construction of the PE

In order to perform ECL measurements, a compact device combining one piece of equipment a potentiostat, and a photodiode integrated into a cell compatible with screen-printed electrodes was used. Hence, the PEs were designed by mimicking screen-printed electrodes and fabricated for the determination of DTZ-HCl. For the construction of the PEs, nitrocellulose membrane (NC) was utilized as a structure, which includes a reaction cell and electrodes. To form the electrochemical reaction cell of the paper electrode, a specific architecture was designed with a thick barrier to provide sealing of the solution. The electrochemical reaction cell was formed to be a 16 mm^2 surface area, by creating the hydrophobic barriers via a wax printer. The resulting wax-pattered NC membrane was shown in Figure 5a. Subsequently, the three electrodes system was created onto the patterned NC membrane. While the construction of the working electrode (WE) and counter electrode (CE) was achieved by using carbon paste, Ag/AgCl paste was used to form the reference electrode (RE). Firstly, a 0.1 mm-steel stencil created by a laser cutter was placed on the patterned NC membrane and then the carbon and Ag/AgCl pastes were applied onto the stencil evenly. Then, the stencil was taken off and the electrodes were created onto the NC membrane surface as shown in Figure 5b. The produced PE was left to dry at ambient temperature overnight and heated to 90°C for 3 minutes to allow the

wax to melt and penetrate the paper membrane layers, and also cure the carbon paste. Ultimately, the copper wire was cut into 4 mm pieces as conductive pads, and they were attached to the electrodes. The overall fabrication procedure was illustrated in Figure 5.

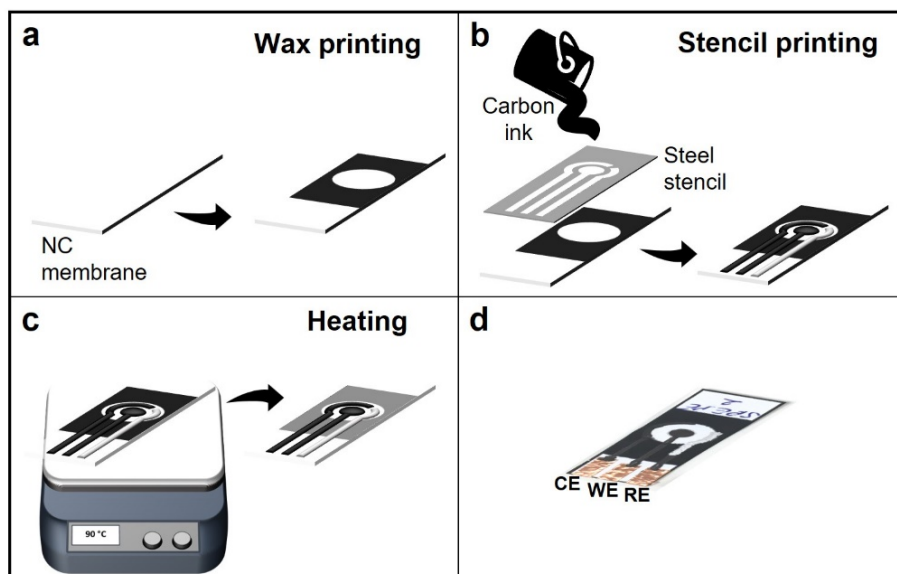


Figure 5. The fabrication procedure of the paper electrode; **a)** the wax printing for preparation of hydrophobic barrier, **b)** the stencil printing to prepare the paper electrode to assemble with CE, WE, and RE, **c)** the heating of the paper electrode, **d)** the photograph of paper electrode assemble

5.3. Surface modification of the PEs

After the fabrication process, the PEs were modified with gold nanoparticles (AuNPs) to enhance ECL signals. The electrodeposition of AuNPs was achieved from 20.0 μL of 0.01 M HAuCl_4 solution including 0.1 M KCl and 0.1 M H_2SO_4 onto the WE surface, using CV in the range of -0.6 to +1.4 V at a scan rate of 200 mV/s for 10 cycles. The AuNPs@PE was activated via a treatment step with phosphate-buffered saline (PBS) solution (pH 7.4) using CV in the range of -1.0 to +1.0 V at a scan rate of 100 mV/s for 3 cycles. The electrochemical characterization of the prepared AuNPs@PEs was achieved using CV. Before and after the modification of PEs, their electrochemical behaviors were monitored by carrying out the CV in the presence of 20.0 μL of 5.0 mM $[\text{Fe}(\text{CN})_6]^{3-/4-}$ a solution containing 0.1 M KCl as a supporting electrolyte, in the range of -0.6 to +0.8 V at a scan rate of 100 mV/s. Furthermore, the morphological properties of the modified PEs were investigated using SEM analysis.

5.4. Sample preparation and the sensing procedure

The standard solutions of DTZ-HCl were prepared at seven different concentrations in the range from 1.0 to 100.0 $\mu\text{g}/\text{mL}$. Initially, the stock solution of DTZ-HCl (2.0 mg/mL) was prepared by dissolving 4.0 mg of DTZ-HCl powder in 2.0 mL of DI water. Then, the stock solution was diluted with DI water to prepare the standard solutions of DTZ-HCl. In order to perform ECL measurements, 10.0 mM $\text{Ru}(\text{bpy})_3^{2+}$ solution was prepared in 100.0 mM TRIS buffer. Here, TRIS buffer was utilized as a supporting electrolyte.

Ten tablets were accurately weighed and crushed to form the powder. The powder including 300 mg of DTZ-HCl was taken into 100.0 mL of DI water. After stirring for 30 min to dissolve DTZ-HCl, the sample solution was filtered through a 0.45 μm nylon-membrane filter. Then the filtered sample solution was diluted to 3 different concentrations. Accordingly, the measurement was performed and the ECL signals were recorded.

Before starting the measurements, the AuNPs@PE was placed onto the top piece of the sensing cell and an o-ring was placed onto the AuNPs@PE to ensure the solution sealing. Then, the bottom piece including a photodiode of the sensing system was covered onto the top piece. The experiment was performed in the following steps: i) the sample solution in a volume of 10.0 μL was applied to the reaction cell of the paper electrode. ii) equal volume of 10.0 mM $\text{Ru}(\text{bpy})_3^{2+}$ solution was dropped into the sample solution onto the paper electrode. iii) The sensor assembled top component of the ECL cell was covered to the bottom component with the paper electrode. iv) In order to generate the excited states of the $\text{Ru}(\text{bpy})_3^{2+}/\text{DTZ}$ pair, the potential in a range from -0.5 to 1.3 V at a scan rate of 100 mV/s was applied by utilizing cyclic voltammetry

(CV) to the AuNRs@PE. iv) Using the μ Stat ECL potentiostat, which is controlled by DropView 8400 Software, the ECL measurements were performed concurrently.

5.5. Optimization studies

In order to investigate the effect of the pH on the ECL intensities, 100.0 μ g/mL DTZ-HCl and 10.0 mM Ru-(bpy)₃²⁺ solutions were prepared in 100.0 mM buffer solutions at eight different pH values in the range from 4.5 to 9.5. For this purpose, three different buffer systems as acetate (pH 4.5-5.5), phosphate (pH 6.5-8.0), and tris (pH 8.5-9.5) buffers were used. The 20.0 μ L of DTZ-HCl and Ru-(bpy)₃²⁺ mixture (1:1 (v/v)) were applied to the reaction cell of AuNPs@PE and then the ECL signals were recorded at the optimum sensing conditions.

The effects of scan rate and different scanning potential ranges on the ECL intensities were investigated in the presence of 20.0 μ L of DTZ-HCl and Ru-(bpy)₃²⁺ mixture (1:1 (v/v)). The concentration of Ru-(bpy)₃²⁺ solution is also crucial for the ECL signal intensities. Therefore, the Ru-(bpy)₃²⁺ solutions at five different concentrations from 1.0 to 20.0 mM were prepared in 100.0 mM TRIS buffer. Then, the ECL signals generated using these solutions were evaluated to determine the optimum concentrations of Ru-(bpy)₃²⁺ solution.

Acknowledgements: This work was partially supported by The Scientific and Technological Research Council of Turkey (TUBITAK) with project number 3001-218S352.

Conflict of interest statement: The author declared no conflict of interest.

REFERENCES

- [1] Deng B, Lu H, Li L, Shi A, Kang Y, Xu Q. 2010; Determination of the number of binding sites and binding constant between diltiazem hydrochloride and human serum albumin by ultrasonic microdialysis coupled with online capillary electrophoresis electrochemiluminescence. *J Chromatogr A*. 1217:4753–4756. [\[CrossRef\]](#)
- [2] Sposito HGM, Lobato A, Tasić N, Maldaner AO, Paixão TRLC, Gonçalves LM. 2022; Swift electrochemical sensing of diltiazem employing highly-selective molecularly-imprinted 3-amino-4-hydroxybenzoic acid. *J Electroanal Chem*. 911:1–7. [\[CrossRef\]](#)
- [3] Ostovar S, Maghsoudi S, Mousavi M. 2021; Development of a sensitive voltammetric sensor for diltiazem determination in biological samples using MWCNT/PPy-PBA modified glassy carbon electrode. *Synth Met*. 281:116928. [\[CrossRef\]](#)
- [4] Salamanca-Neto CAR, Felsner ML, Galli A, Sartori ER. 2019; In-house validation of a totally aqueous voltammetric method for determination of diltiazem hydrochloride. *J Electroanal Chem*. 837:159–166. [\[CrossRef\]](#)
- [5] Imani R, Shabani-Nooshabadi M, Ziaie N. 2022; Fabrication of a sensitive sensor for electrochemical detection of diltiazem in presence of methyl dopa. *Chemosphere*. 297:134170. [\[CrossRef\]](#)
- [6] USP. 2017; U.S. Pharmacopoeia-National Formulary [USP 40 NF 35], United States Pharmacopoeial Convention, Rockville, Md
- [7] Fiorentin TR, Logan BK, Martin DM, Browne T, Rieders EF. 2020; Assessment of a portable quadrupole-based gas chromatography mass spectrometry for seized drug analysis. *Forensic Sci Int*. 313:110342. [\[CrossRef\]](#)
- [8] Sanchez MA, Rocha FRP. 2011; Liquid-liquid microextraction without phase separation in a multicommutated flow system for diltiazem determination in pharmaceuticals. *Anal Chim Acta*. 694:95–99. [\[CrossRef\]](#)
- [9] Li N, He S, Li C, Yang F, Dong Y. 2021; Sensitive Analysis of Metoprolol Tartrate and Diltiazem Hydrochloride in Human Serum by Capillary Zone Electrophoresis Combining on Column Field-Amplified Sample Injection. *J Chromatogr Sci*. 59:465–472. [\[CrossRef\]](#)
- [10] Wu HY, Cunningham BT. 2014; Point-of-care detection and real-time monitoring of intravenously delivered drugs via tubing with an integrated SERS sensor. *Nanoscale*. 6:5162–5171. [\[CrossRef\]](#)
- [11] Ayad MM, Shalaby A, Abdellatef HE, Hosny MM. 2003; New colorimetric methods for the determination of trazodone HCl, famotidine, and diltiazem HCl in their pharmaceutical dosage forms.

- Anal Bioanal Chem. 376:710–714. [\[CrossRef\]](#)
- [12] Rahman N, Azmi SNH. 2000; Spectrophotometric determination of diltiazem hydrochloride with sodium metavanadate. *Microchem J.* 65:39–43. [\[CrossRef\]](#)
- [13] Torul H, Gumustas M, Urguplu B, Uzunoglu A, Boyaci IH, Celikkan H, Tamer U. 2021; Disposable electrochemical flow cell with paper-based electrode assemble. *J Electroanal Chem.* 891:115268. [\[CrossRef\]](#)
- [14] Torul H, Yarali E, Eksin E, Ganguly A, Benson J, Tamer U, Papakonstantinou P, Erdem A. 2021; Paper-based electrochemical biosensors for voltammetric detection of miRNA biomarkers using reduced graphene oxide or MoS₂ nanosheets decorated with gold nanoparticle electrodes. *Biosensors.* 11:236. [\[CrossRef\]](#)
- [15] Adsetts JR, Chu K, Hesari M, Ma J, Ding Z. 2021; Absolute Electrochemiluminescence Efficiency Quantification Strategy Exemplified with Ru(bpy)₃²⁺ in the Annihilation Pathway. *Anal Chem.* 93:11626–11633. [\[CrossRef\]](#)
- [16] Li L, Chen Y, Zhu J. 2017; Recent Advances in Electrochemiluminescence Analysis. *Anal Chem.* 89:358–371. [\[CrossRef\]](#)
- [17] Kirschbaum SEK, Baeumner AJ. 2015; A review of electrochemiluminescence (ECL) in and for microfluidic analytical devices. *Anal Bioanal Chem.* 407:3911–3926. [\[CrossRef\]](#)
- [18] Liu Y, Guo W, Su B. 2019; Recent advances in electrochemiluminescence imaging analysis based on nanomaterials and micro- / nanostructures. *Chinese Chem Lett J.* 30:1593–1599. [\[CrossRef\]](#)
- [19] Wang X, Liu H, Qi H, Gao Q, Zhang C. 2020; Highly efficient electrochemiluminescence of ruthenium complex-functionalized CdS quantum dots and their analytical application. *J Mater Chem B.* 8:3598–3605. [\[CrossRef\]](#)
- [20] Wang H, Chai Y, Li H, Yuan R. 2018; Sensitive electrochemiluminescent immunosensor for diabetic nephropathy analysis based on tris(bipyridine) ruthenium(II) derivative with binary intramolecular self-catalyzed property. *Biosens Bioelectron.* 100:35–40. [\[CrossRef\]](#)
- [21] Zhang A, Guo W, Ke H, Zhang X, Zhang H, Huang C, Yang D, Jia N, Cui D. 2018; Sandwich-format ECL immunosensor based on Au star@BSA-Luminol nanocomposites for determination of human chorionic gonadotropin. *Biosens Bioelectron.* 101:219–226. [\[CrossRef\]](#)
- [22] Ma C, Yue C, Xiaodan G, Jun-Jie Z. 2020; Recent Progress in Electrochemiluminescence Sensing and Imaging. *Anal Chem.* 92:431–454. [\[CrossRef\]](#)
- [23] Yuan F, Hao K, Sheng S, Haile T, Ma X, Xu G. 2020; 2-(Dibutylamino) ethyl acrylate as a highly efficient co-reactant of 3 electrochemiluminescence for selective detection of cysteine. *Electrochim Acta.* 329:135117. [\[CrossRef\]](#)
- [24] Miao W, Choi J, Bard AJ. 2002; Electrogenerated Chemiluminescence 69: The Tri-n-propylamine (TPRA) System Revisited-A New Route Involving TPRA^{•+} + Cation Radicals. *J Am Chem Soc.* 124:14478–14485. [\[CrossRef\]](#)
- [25] Liu C, Song D, Yang Z, Wang Z, Pan P, Liu J, Yang X, Li R, Zhu Z, Xue F. 2021; Research on advanced methods of electrochemiluminescence detection combined with optical imaging analysis for the detection of sulfonamides. *Analyst.* 146:7611–7617. [\[CrossRef\]](#)
- [26] Ge L, Yu J, Ge S, Yan M. 2014; Lab-on-paper-based devices using chemiluminescence and electrogenerated chemiluminescence detection. *Anal Bioanal Chem.* 406:5613–5630. [\[CrossRef\]](#)
- [27] Zheng W, Wang K, Xu H, Zheng C, Cao B, Qin Q, Jin Q, Cui D. 2021; Strategies for the detection of target analytes using microfluidic paper-based analytical devices. *Anal Bioanal Chem.* 413:2429–2445. [\[CrossRef\]](#)
- [28] Noviana E, McCord CP, Clark KM, Jang I, Henry CS. 2020; Electrochemical paper-based devices: Sensing approaches and progress toward practical applications. *Lab Chip.* 20:9–34. [\[CrossRef\]](#)
- [29] Liu Y, Liu Y, Qiao L, Liu Y, Liu B. 2018; Advances in signal amplification strategies for electrochemical biosensing. *Curr Opin Electrochem.* 12:5–12. [\[CrossRef\]](#)
- [30] Husain RA, Barman SR, Chatterjee S, Khan I, Lin ZH. 2020; Enhanced biosensing strategies using

- electrogenerated chemiluminescence: recent progress and future prospects. *J Mater Chem B*. 8:3192–3212. [\[CrossRef\]](#)
- [31] Zhao C, Niu L, Wang X, Sun W. 2019; Small Size Effect and Concentration Response of Gold Nanoparticles in Electrochemiluminescence Reaction. *Electroanalysis*. 31:1752–1757. [\[CrossRef\]](#)
- [32] Zhao C, Niu L, Wang X, Sun W. 2018; Electrochemiluminescence of gold nanoparticles and gold nanoparticle-labelled antibodies as co-reactants. *RSC Adv*. 8:36219–36222. [\[CrossRef\]](#)
- [33] Eksin E, Torul H, Yarali E, Tamer U, Papakonstantinou P, Erdem A. 2021; Paper-based electrode assemble for impedimetric detection of miRNA. *Talanta*. 225:122043. [\[CrossRef\]](#)
- [34] Yarali E, Eksin E, Torul H, Ganguly A, Tamer U, Papakonstantinou P, Erdem A. 2022; Impedimetric detection of miRNA biomarkers using paper-based electrodes modified with bulk crystals or nanosheets of molybdenum disulfide. *Talanta*. 241:123233. [\[CrossRef\]](#)
- [35] Mahajan N, Deshmukh S, Farooqui M. 2021; A novel stability-indicating method for known and unknown impurities profiling for diltiazem hydrochloride pharmaceutical dosage form (tablets). *Futur J Pharm Sci*. 7:1–13. [\[CrossRef\]](#)

This is an open access article which is publicly available on our journal's website under Institutional Repository at <http://dspace.marmara.edu.tr>.